JACS
JOURNAL OF THE AMERICAN CHEMICAL SOCIETY
Communication
pubs.acs.org/JACS

Graphene Oxide Based Recyclable Dehydrogenation of Ammonia Borane within a Hybrid Nanostructure

Ziwei Tang,† Hao Chen,† Xiaowei Chen, Limin Wu,* and Xuebin Yu*

Department of Materials Science, Fudan University, Shanghai 200433, China

Supporting Information

ABSTRACT: The recyclable dehydrogenation of ammonia borane (AB) is achievable within a graphene oxide (GO)-based hybrid nanostructure, in which a combined modification strategy of acid activation and nanoconfinement by GO allows AB to release more than 2 equiv of pure H_2 at temperatures below 100 °C. This process yields polyborazylene (PB) as a single product and, thus, promotes the chemical regeneration of AB via reaction of PB with hydrazine in liquid ammonia.

One indispensable target in the development of a hydrogen-based energy substructure is the storage and controlled distribution of hydrogen. Various hydrogen storage methodologies are currently under examination, including chemical hydrides,[1] sorbents,[2] and metal hydrides.[3] Among them, ammonia borane (NH_3BH_3, AB) continues to be one of the most promising media for a chemical hydride-based hydrogen storage system suitable for portable applications.[4] It has shown satisfactory air stability and remarkably high energy-storage density (gravimetric and volumetric hydrogen capacities are 19.6 wt % and 140 $g{\cdot}L^{-1}$, respectively), and it has recently been shown to be regenerable from its spent fuel.[5] However, the direct use of pristine AB as a hydrogen energy carrier in on-board applications is impeded by its sluggish dehydrogenation kinetics below 100 °C and by the concurrent evolution of a large amount of detrimental volatile byproduct, including borazine, ammonia, and diborane, which not only poisons the catalyst of the proton membrane fuel cell but also causes irrecoverable component loss (B and N elements) during the dehydrogenation process, dramatically degrading regeneration efficiency.[6] Currently, several methods have been adopted to promote the efficient release of pure H_2 from AB, including initiation by acids,[7] bases,[8] ion liquids,[9] transition-metal catalysts,[10] and nanoscaffolds.[11] These initial advances led us to expect that the combination of aforementioned activation strategies of dehydrogenation in AB would allow the further enhancement of its hydrogen storage performance.

A recent breakthrough research study has demonstrated the successful conversion of polyborazylene (PB) to AB via reaction with hydrazine in liquid ammonia, in which the PB was derived from the dehydrogenation of borazine for a purer form. It indicates that giving PB as a single spent-fuel component of AB is a crucial factor for facilitating efficient AB regeneration.[5c] The route conversion of AB to PB has often been performed using metal catalysts,[12] which seems to offer a potentially feasible pathway toward direct AB recycling through metal-catalyzed AB dehydrogenation. However, the presence of a residual metal catalyst in PB mixtures could complicate the AB regeneration process.[5c] One recent work further demonstrated that a metal-catalyst-free conversion of AB to PB could be realized upon treatment with a proton acceptor, which deprotonated AB to form the $H_3BNH_2^-$ anion that then initiated the AB dehydrocoupling H_2-release process.[8a] Because AB contains both protonic and hydridic hydrogens, it is also likely to react with a proton donor to yield the $H_3NBH_2^+$ cation.[7] Thus, it is supposed that an approach to PB from AB would be activated via AB cationic dehydropolymerization as well.

Graphene oxide (GO), which possesses the characteristics of graphene, shows great promise for the fabrication of nanoscale structures[13] and, more importantly, contains a range of reactive oxygen functional groups (e.g., hydroxyl groups) via chemical modification or functionalization of its carbon backbone.[14] It, therefore, can serve as an AB supporter that renders the cationic initiation of AB dehydropolymerization using its hydroxyl as the proton donor and to improve AB dehydrogenation through the nanoconfinement effect within its substantially layered nanostructure. Nevertheless, reports on the use of GO in chemical hydrogen storage have been rare.[15]

On the basis of the above assumptions and the results of the following experiments, a mechanism to interpret the formation of the GO-AB hybrid nanostructure is put forward. It is shown in Figure 1. GO sheets have their basal planes decorated mostly with hydroxyl groups.[16] These groups enable the protonolysis of the B−H bond in some of the AB molecules, which were introduced in between the separated GO sheets by solvent. This causes the formation of cationic AB attached to the negatively charged oxygen via an electrostatic effect (Figure 1b). While concomitantly introduced other AB molecules are unprotonated and distributed within the interlayer space, and GO sheets are prone to restacking to create a sandwiched GO-AB-GO structure as the solvent was removed. AB and its cationic initiator became coencapsulated inside the GO interlayer. The ^{11}B NMR chemical shift (−11.6 ppm, Figure S1) was consistent with its DFT calculated value (−11.5 ppm) for AB cations in GO-AB nanocomposites (30 and 50 wt % AB loaded samples denoted as GAB30 and GAB50, respectively). This provides direct support for the GO/AB reaction. However, the sample prepared from mechanically mixing two starting materials (30 wt % AB, denoted as MGAB) only showed the AB resonance signal, suggesting that no interaction

Received: January 1, 2012
Published: March 14, 2012

dx.doi.org/10.1021/ja300003t | J. Am. Chem. Soc. 2012, 134, 5464−5467

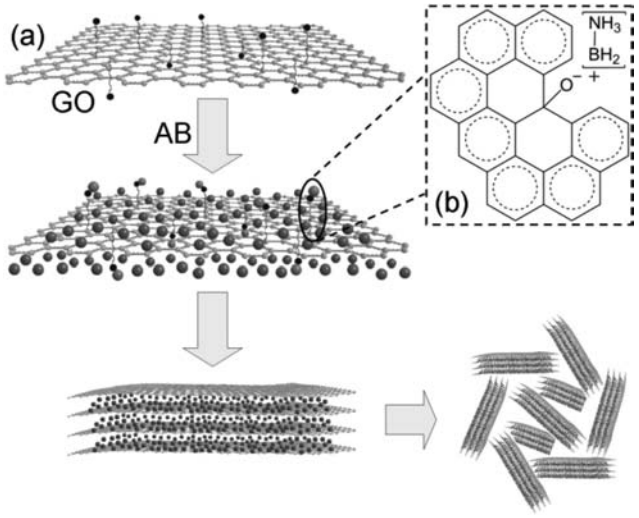

Figure 1. (a) Schematic representation of the mechanism of the formation of GO-AB hybrid nanostructure. (b) The detailed illustration of interaction between AB cation and negatively charged oxygen of GO.

between GO and AB occurred in the surface-contacted mixing mode. This is similar to other AB nanocomposite systems.[17]

The cross-section of GAB30 has a honeycomb-like structure, as shown by scanning electron microscopy (SEM, Figure 2a

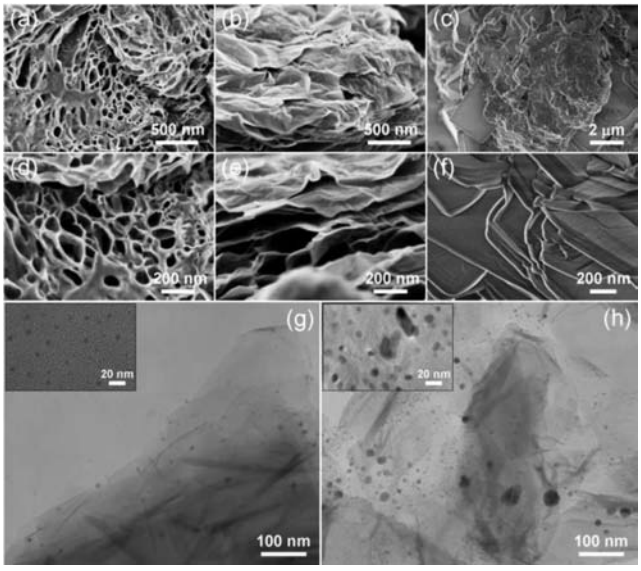

Figure 2. SEM images of (a) GAB30, (b) GAB50, (c) MGAB, and (f) GO. High-magnification (d, e) SEM and (g, h) TEM images of (d, g) GAB30 and (e, h) GAB50 (the insets of images g and h are the corresponding high-resolution TEM micrographs).

and 2d). This is caused by insufficient AB medium within the GO interlayer space, leading to restacking of the partial GO sheets. As the AB content in the GO interlayer increases, the layered structure of GO is retained, as shown by the SEM image of GAB50 (Figure 2b and 2e). This suggests that numerous AB particles work as sheet spacers. Without spacers in the GO interlayer (Figure 2c and 2f), the sheets undergo visible agglomeration, and AB particles aggregate extensively along with the agglomerated GO sheets in the physically mixed sample of MGAB (Figure 2c). To assess the distribution of AB particles in the samples, we performed transmission electronic microscopy (TEM). As can be seen from Figure 2g and 2h, AB particles are uniformly spread throughout the GO sheets with the average diameters of 4 and 10 nm (insets and Figure S2) in GAB30 and GAB50, respectively, indicating that a decreasing concentration of AB in GO causes smaller grains. The BET surface area and total pore volume of GO are decreased from 391 to 255, 104, and 67 $m^2 \cdot g^{-1}$, and from 2.85 to 2.17, 0.65, and 0.42 $cm^3 \cdot g^{-1}$, respectively for MGAB, GAB30, and GAB50, further confirming that AB particles occupy the interlayer space of GO in GAB30 and GAB50 and accumulate on the GO surface in MGAB. This was also demonstrated via the N_2 adsorption−desorption (Figure S3) and X-ray diffraction (Figure S4) measurements.

The comparison of the thermal decomposition properties of GAB30, GAB50, MGAB, and neat AB was performed using mass spectrometry (MS), as shown in Figures 3a and S5. Neat

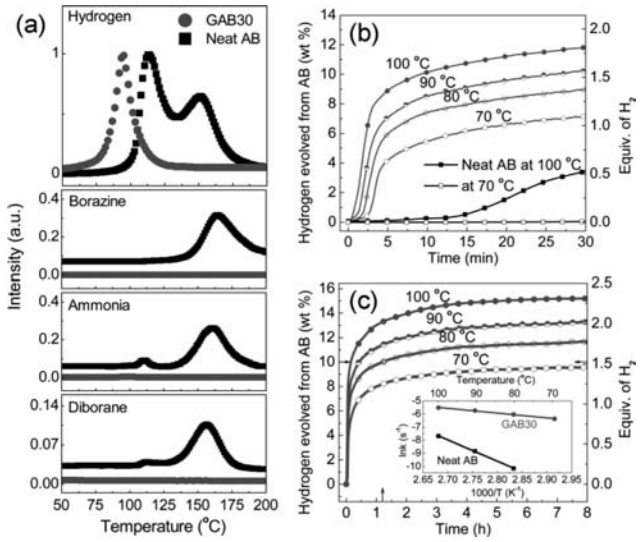

Figure 3. (a) Mass spectra of GAB30 and neat AB with a heating rate of 5 °C·min^{-1}. (b) Isothermal TPD and (c) time-extended results of hydrogen released from AB in GAB30 at 70, 80, 90, and 100 °C (GO was not considered an active component during the measurements. The inset of (c) is Arrhenius treatment of the temperature-dependent rate data that gives the activation energy of neat AB and GAB30).

AB dehydrogenates at temperatures above 100 °C. It emits toxic gases such as borazine, ammonia, and diborane during the second step. GAB50, however, has a reduced onset H_2-release temperature of 67 °C and a two-step dehydrogenation with peaks centered at 99 and 125 °C. It also significantly suppresses the emission of all kinds of impurities. The starting and peak temperatures of H_2 evolution in GAB30 are considerably decreased, to 50 and 94 °C, respectively, and the simultaneously evolved byproduct gases are completely depressed. This suggests that nanoconfinement effects improve performance in samples with low AB content. However, no obvious improvement of dehydrogenation was detected in physically mixed MGAB samples. This further demonstrates that the combined effect of nanoconfinement and cationic activation of AB that stems from the interlayer of GO plays a crucial role in advancing the release of H_2 from the hybrid structure. This was also indicated by the thermogravimetry (TG) characterization (Figure S6), where the weight loss in GAB30 is less than that of GAB50 and much less than that of MGAB or neat AB. The

dx.doi.org/10.1021/ja300003t | J. Am. Chem. Soc. 2012, 134, 5464−5467

differential scanning calorimetry (DSC) results (Figure S7) show that the melting points, exothermic peaks (corresponding to the hydrogen evolution), and reaction enthalpies of GAB30 and GAB50 are dramatically decreased relative to those of MGAB and neat AB, which is attributed to the nanoscale effect.[18]

Given that GAB30 performed with the best thermodynamics, we further studied its isothermal H_2 release property by employing the volumetric temperature programmed desorption (TPD), as depicted in Figure 3b. The GAB30 sample could generate 10.1 wt % H_2 (1.54 equiv) at 100 °C in 10 min and reach 11.8 wt % (1.80 equiv) within 30 min; by comparison, the neat AB merely released 3.4 wt % H_2 (0.51 equiv) under the same conditions. At a lower temperature of 70 °C, about 7.2 wt % (1.09 equiv) hydrogen evolution could be implemented within 30 min in GAB30, while no hydrogen was liberated from the neat AB. Time-prolonged isothermal measurements (Figure 3c) indicate that GAB30 presents a more than 10 wt % H_2 liberation within 1.2 h at 80 °C (1.52 equiv). This exceeds recently reported solid-state AB systems with respect to rate and the extent of H_2 release[19] and is comparable with that of some ion liquid-relative systems.[9,20] For a better exploration of the kinetic properties, the activation energies have been calculated from various isotherm curves (Figures 3c and S8) through Arrhenius treatment. From the slope of the linear plot of ln k (k, rate constant) versus $1/T$ (T, absolute temperature), the apparent activation energies for H_2 loss from neat AB and GAB30 were found to be 135.0 and 30.4 kJ·mol^{-1}, respectively (Figure 3c). This distinctly validates the kinetic enhancement.

In order to find insight into the pathway of dehydrogenation from GAB30, solid-state ^{11}B NMR was used to monitor the GO/AB reactions at different stages. Association with both the H_2-release measurements and the ^{11}B NMR studies of the solid-state GO/AB reactions, the spectrum (Figure 4a(i)) of

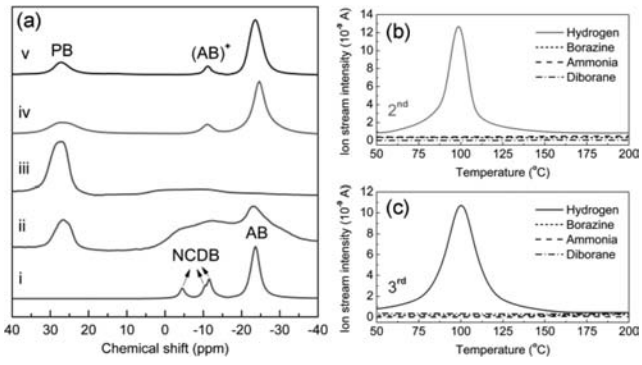

Figure 4. (a) Solid-state ^{11}B NMR spectra of GAB30 after the release of H_2: (i) 0.63 equiv, (ii) 1.09 equiv, (iii) 2.31 equiv, and (iv) the first and (v) the second regenerated product of dehydrogenated GAB30. (b) and (c) are the MS results for the second and third dehydrogenation cycles of GAB30.

GAB30 shows, after 0.63 equiv of H_2 was released, the resonances of both unreacted AB (−23.5 ppm) and cationic *N*-(cyclodiborazanyl)boranamine (NCDB; −4.5, −10.7, and −11.5 ppm). This was validated by ^{11}B NMR chemical shift calculations. As the reaction proceeded (Figure 4a(ii)), the resonances broadened and diminished, and a new resonance appeared centered at 26.6 ppm. This is a feature of the unsaturated sp^2-hybridized boron framework of the cross-linked PB structure.[21] Further dehydrogenation at 100 °C for 8 h resulted in 2.31 equiv of H_2 evolving from GAB30, which produces PB as the final product (Figure 4a(iii)). The cationic AB, which is chemically similar to the diammoniate of diborane (DADB), has been implicated as the reaction initiator in acid-activated dehydrocoupling of AB.[7] In this way, these cations can permit the facile release of H_2 by the intermolecular reaction of hydridic B−H hydrogens with N−H protons on itself and an adjacent AB molecule to form polyaminoborane (PAB)-homologized NCDB cations, which then continue the intermolecular dehydrocoupling with AB molecules and/or cyclize to cationic cyclodiborazane (CDB). Finally, these intermediates, which were obtained by the evolution of 1 equiv of H_2 from AB, emitted more than 1 equiv of H_2 to produce unsaturated cross-linked PB material. This supposed cationic polymerization pathway for GO-induced H_2 release from AB is illustrated in Figure S9. It is similar to that of base-initiated reactions of AB.

AB was regenerated by allowing the direct decomposition product of GAB30 to react with hydrazine in liquid ammonia, as described recently.[5c] This was verified by ^{11}B NMR (Figure 4a(iv)). During this process, the hydroxyl groups on the GO sheets were reproduced simultaneously (cationic AB reappears). This affords sustainable support for AB recycling dehydrogenation within the GO interlayer, as illustrated in Figure S10.[22] MS investigation of the first hydrogenated product (Figure 4b) shows results identical to those found for the as-prepared GAB30 (Figure 3a). Similar results were also observed after its second de/rehydrogenation cycle (Figures 4a(v) and 4c), providing evidence of the recyclability of GAB30. However, some PB does remain in the system upon cycling. This may be attributed to the inaccessible interaction between reductants and tightly encapsulated PB inside the GO. TG analysis of the rehydrogenated products indicates that 71% and 65% of AB was successfully recycled for the first and second regeneration process, respectively (Figure S11). The second regeneration efficiency was around 91% of the first one, which verified that internally unreacted PB dominates the cycling loss.

Many studies of AB chemistry have concentrated on the decomposition of this compound, especially with respect to its ability to rapidly release H_2. Here, we have shown that our new process, which establishes direct chemical cycles for AB dehydrogenation, is a valid approach toward the recycling of AB. This method may constitute an advancement in the practical application for AB as a hydrogen storage candidate. In this study, GO was shown to be the nanoscaffold as well as a proton donor. Thus, it caused AB to release more than 2 equiv of H_2 (corresponding 15.2 wt % of the loaded AB) to form PB as a single product without the formation of any gas byproducts. This warranted the sustainability of a cyclic procedure and facilitated AB regeneration. Moreover, after the second cycle, the regenerated AB continued to exhibit superior dehydrogenation performance. Our findings suggest that constructing a chemically modified AB system with advanced H_2 release and recyclability may require the adoption of synergistic optimization strategies. For this route to become a commercially viable means of portable H_2 storage, however, we must address issues including low content of the active component of AB in the system and diminutions in productivity after multiple regenerations. These concerns might be surmounted through seeking alternative supporters or matrixes with more flexible internal environments, which

dx.doi.org/10.1021/ja300003t | J. Am. Chem. Soc. 2012, 134, 5464−5467

would increase the loading rate and contact area between PB and reductants. Furthermore, we think that the prospective exploitations of recyclability of AB and even other B−N hydrogen storage materials should be focused on the following: (i) orientation of reaction pathway to obtain single final product by adding catalysts or activators; (ii) development of new chemical reduction techniques to facilitate and simplify the regeneration procedure, which will promote these B−N-based systems to approach a real on-board application. Nevertheless, finding solutions to these issues still remains a big challenge.

■ ASSOCIATED CONTENT

Supporting Information

Full experimental procedures and characterization details. This material is available free of charge via the Internet at http://pubs.acs.org.

■ AUTHOR INFORMATION

Corresponding Author

yuxuebin@fudan.edu.cn; lmw@fudan.edu.cn

Author Contributions

†These authors contributed equally to this work.

Notes

The authors declare no competing financial interest.

■ ACKNOWLEDGMENTS

This work was partially supported by the Ministry of Science and Technology of China (2010CB631302), the National Natural Science Foundation of China (Grant No. 51071047, 51133001), the PhD Programs Foundation of Ministry of Education of China (20110071110009, 20110071130002), and the Science and Technology Commission of Shanghai Municipality (11JC1400700, 11520701100, 10JC1401900).

■ REFERENCES

(1) (a) Orimo, S.; Nakamori, Y.; Eliseo, J. R.; Zuttel, A.; Jensen, C. M. *Chem. Rev.* **2007**, *107*, 4111. (b) Hamilton, C.; Baker, R.; Staubitz, A.; Manners, I. *Chem. Soc. Rev.* **2009**, *38*, 279. (c) Liu, X.; McGrady, G. S.; Langmi, H. W.; Jensen, C. M. *J. Am. Chem. Soc.* **2009**, *131*, 5032.

(2) (a) Pan, L.; Sander, M. B.; Huang, X. Y.; Li, J.; Smith, M.; Bittner, E.; Bockrath, B.; Johnson, J. K. *J. Am. Chem. Soc.* **2004**, *126*, 1308. (b) Yang, R. T.; Wang, Y. *J. Am. Chem. Soc.* **2009**, *131*, 4224.

(3) (a) Grochala, W.; Edwards, P. P. *Chem. Rev.* **2004**, *104*, 1283. (b) Graetz, J. *Chem. Soc. Rev.* **2009**, *38*, 73.

(4) (a) Stephens, F. H.; Pons, V.; Baker, R. T. *Dalton Trans.* **2007**, 2613. (b) Marder, T. B. *Angew. Chem., Int. Ed.* **2007**, *46*, 8116. (c) Peng, B.; Chen, J. *Energy Environ. Sci.* **2008**, *1*, 479. (d) Smythe, N. C.; Gordon, J. C. *Eur. J. Inorg. Chem.* **2010**, *2010*, 509. (e) Staubitz, A.; Robertson, A. P. M; Sloan, M. E.; Manners, I. *Chem. Rev.* **2010**, *110*, 4023. (f) Staubitz, A.; Robertson, A. P. M; Manners, I. *Chem. Rev.* **2010**, *110*, 4079.

(5) (a) Davis, B. L.; Dixon, D. A.; Garner, E. B.; Gordon, J. C.; Matus, M. H.; Scott, B.; Stephens, F. H. *Angew. Chem., Int. Ed.* **2009**, *48*, 6812. (b) Sutton, A. D.; Davis, B. L.; Bhattacharyya, K. X.; Ellis, B. D.; Gordon, J. C.; Power, P. P. *Chem. Commun.* **2010**, *46*, 148. (c) Sutton, A. D.; Burrell, A. K.; Dixon, D. A.; Garner, E. B. III; Gordon, J. C.; Nakagawa, T.; Ott, K. C.; Robinson, J. P.; Vasiliu, M. *Science* **2011**, *331*, 1426.

(6) Yang, J.; Sudik, A.; Wolverton, C. *Chem. Soc. Rev.* **2010**, *39*, 656.

(7) Stephens, F. H.; Baker, R. T.; Matus, M. H.; Grant, D. J.; Dixon, D. A. *Angew. Chem., Int. Ed.* **2007**, *46*, 746.

(8) (a) Himmelberger, D.; Yoon, C.; Bluhm, M.; Carroll, P.; Sneddon, L. *J. Am. Chem. Soc.* **2009**, *131*, 14101. (b) Ewing, W. C.; Marchione, A.; Himmelberger, D. W.; Carroll, P. J.; Sneddon, L. G. *J. Am. Chem. Soc.* **2011**, *133*, 17093.

(9) (a) Bluhm, M. E.; Bradley, M. G.; Butterick, R. III; Kusari, U.; Sneddon, L. G. *J. Am. Chem. Soc.* **2006**, *128*, 7748. (b) Himmelberger, D. W.; Alden, L. R.; Bluhm, M. E.; Sneddon, L. G. *Inorg. Chem.* **2009**, *48*, 9883.

(10) (a) Jaska, C. A.; Temple, K.; Lough, A. J.; Manners, I. *J. Am. Chem. Soc.* **2003**, *125*, 9424. (b) Staubitz, A.; Sloan, M. E.; Robertson, A. P.; Friedrich, A.; Schneider, S.; Gates, P. J.; Schmedt auf der Gunne, J.; Manners, I. *J. Am. Chem. Soc.* **2010**, *132*, 13332. (d) Conley, B. L.; Guess, D.; Williams, T. J. *J. Am. Chem. Soc.* **2011**, *133*, 14212.

(11) (a) Gutowska, A.; Li, L. Y.; Shin, Y. S.; Wang, C. M. M.; Li, X. H. S.; Linehan, J. C.; Smith, R. S.; Kay, B. D.; Schmid, B.; Shaw, W.; Gutowski, M.; Autrey, T. *Angew. Chem., Int. Ed.* **2005**, *44*, 3578. (b) Kim, H.; Karkamkar, A.; Autrey, T.; Chupas, P.; Proffen, T. *J. Am. Chem. Soc.* **2009**, *131*, 13749. (c) Li, Y. Q.; Song, P.; Zheng, J.; Li, X. G. *Chem.—Eur. J.* **2010**, *16*, 10887.

(12) Keaton, R. J.; Blacquiere, J. M.; Baker, R. T. *J. Am. Chem. Soc.* **2007**, *129*, 1844.

(13) (a) Kosynkin, D. V.; Higginbotham, A. L.; Sinitskii, A.; Lomeda, J. R.; Dimiev, A.; Price, B. K.; Tour, J. M. *Nature* **2009**, *458*, 872. (b) Allen, M. J.; Tung, V. C.; Kaner, R. B. *Chem. Rev.* **2009**, *110*, 132.

(14) (a) Stankovich, S.; Dikin, D. A.; Dommett, G. H. B.; Kohlhaas, K. M.; Zimney, E. J.; Stach, E. A.; Piner, R. D.; Nguyen, S. T.; Ruoff, R. S. *Nature* **2006**, *442*, 282. (b) Dikin, D. A.; Stankovich, S.; Zimney, E. J.; Piner, R. D.; Dommett, G. H. B.; Evmenenko, G.; Nguyen, S. T.; Ruoff, R. S. *Nature* **2007**, *448*, 457.

(15) Subrahmanyam, K. S.; Kumar, P.; Maitra, U.; Govindaraj, A.; Hembram, K. P.; Waghmare, U. V.; Rao, C. N. *Proc. Natl. Acad. Sci. U.S.A.* **2011**, *108*, 2674.

(16) Dreyer, D. R.; Park, S.; Bielawski, C. W.; Ruoff, R. S. *Chem. Soc. Rev.* **2010**, *39*, 228.

(17) (a) Sepehri, S.; Feaver, A.; Shaw, W. J.; Howard, C. J.; Zhang, Q.; Autrey, T.; Cao, G. *J. Phys. Chem. B* **2007**, *111*, 14285. (b) Neiner, D.; Luedtke, A.; Karkamkar, A.; Shaw, W.; Wang, J.; Browning, N. D.; Autrey, T.; Kauzlarich, S. M. *J. Phys. Chem. C* **2010**, *114*, 13935.

(18) (a) Li, S. F.; Guo, Y. H.; Sun, W. W.; Sun, D. L.; Yu, X. B. *J. Phys. Chem. C* **2010**, *114*, 21885. (b) Tang, Z. W.; Li, S. F.; Yang, Z. X.; Yu, X. B. *J. Mater. Chem.* **2011**, *21*, 14616.

(19) (a) Li, Z.; Zhu, G.; Lu, G.; Qiu, S.; Yao, X. *J. Am. Chem. Soc.* **2010**, *132*, 1490. (b) Gadipelli, S.; Ford, J.; Zhou, W.; Wu, H.; Udovic, T. J.; Yildirim, T. *Chem.—Eur. J.* **2011**, *17*, 6043.

(20) Wright, W. R.; Berkeley, E. R.; Alden, L. R.; Baker, R. T.; Sneddon, L. G. *Chem. Commun.* **2011**, *47*, 3177.

(21) (a) Fazen, P. J.; Beck, J. S.; Lynch, A. T.; Remsen, E. E.; Sneddon, L. G. *Chem. Mater.* **1990**, *2*, 96. (b) Fazen, P. J.; Remsen, E. E.; Beck, J. S.; Carroll, P. J.; McGhie, A. R.; Sneddon, L. G. *Chem. Mater.* **1995**, *7*, 1942.

(22) Peng, X. Y.; Liu, X. X.; Diamond, D.; Lau, K. T. *Carbon* **2011**, *49*, 3488.